

# Targeting miR-21 for the Therapy of Pancreatic Cancer

Flavie Sicard<sup>1,2</sup>, Marion Gayral<sup>1,2</sup>, Hubert Lulka<sup>1,2</sup>, Louis Buscail<sup>1,2</sup> and Pierre Cordelier<sup>1,2</sup>

<sup>1</sup>INSERM U1037, Cancer Research Center of Toulouse, Toulouse, France; <sup>2</sup>Université Paul Sabatier Toulouse III, Toulouse, France

Despite tremendous efforts worldwide from clinicians and cancer scientists, pancreatic ductal adenocarcinoma (PDA) remains a deadly disease for which no cure is available. Recently, microRNAs (miRNAs) have emerged as key actors in carcinogenesis and we demonstrated that microRNA-21 (miR-21), oncomiR is expressed early during PDA. In the present study, we asked whether targeting miR-21 in human PDA-derived cell lines using lentiviral vectors (LVs) may impede tumor growth. We demonstrated that LVs-transduced human PDA efficiently downregulated miR-21 expression, both *in vitro* and *in vivo*. Consequently, cell proliferation was strongly inhibited and PDA-derived cell lines died by apoptosis through the mitochondrial pathway. *In vivo*, miR-21 depletion stopped the progression of a very aggressive model of PDA, to induce cell death by apoptosis; furthermore, combining miR-21 targeting and chemotherapeutic treatment provoked tumor regression. We demonstrate herein for the first time that targeting oncogenic miRNA strongly inhibit pancreatic cancer tumor growth both *in vitro* and *in vivo*. Because miR-21 is overexpressed in most human tumors; therapeutic delivery of miR-21 antagonists may still be beneficial for a large number of cancers for which no cure is available.

Received 23 August 2012; accepted 30 January 2013; advance online publication 12 March 2013. doi:10.1038/mt.2013.35

## INTRODUCTION

The vast majority of patients with pancreatic ductal adenocarcinoma (PDA) display an advanced disease that results in a low resection rate leading to a dismal overall median survival of 4–6 months.<sup>1</sup> The estimated 5-year survival rate is <5%. Although PDA is not among the most common tumors, it is one of the most frequent causes of cancer-related death with ~28,000 deaths/year in the United States and 40,000/year in Europe.<sup>1</sup> The therapeutic armamentarium against PDA consists of conventional chemotherapeutic agents such as gemcitabine and more recently FOLFIRINOX that offer a marginal survival benefit for PDA patients.<sup>2,3</sup> Moreover, unlike other digestive cancer entities such as colon cancer or gastrointestinal stromal tumors, molecular-targeted therapies have so far largely failed to positively impact patient survival in PDA.<sup>2</sup> Consequently, developing new

treatments that may profoundly change the therapeutic landscape of PDA is urgently needed.

For the vast majority, PDA occurs sporadically. Milestone genetic studies identified *K-ras* gene activation in >85% of PDAs, whereas *p16* and *TP53* are inactivated in about 95% of cases.<sup>2</sup> Last, *SMAD4* is lost in 55% of PDAs. By contrast, little is known about the subsequent molecular changes contributing to this very aggressive cancer. Many growth signaling pathways are over-activated in PDA while alteration of tumor suppressor gene expression is frequently detected in PDA. Consequently, evasion of apoptosis, cell survival, aberrant angiogenesis, invasion, and metastatic spread are landmarks of PDA. In addition, many other processes are involved in PDA and can contribute to its development. Much progress has been made linking the expression of microRNAs (miRNA) with PDA.<sup>4</sup> Despite their small size at about 22 nucleotides, these endogenous noncoding RNAs have an astonishing effect on protein-coding gene expression, and regulate various cellular events including proliferation, apoptosis, and differentiation.<sup>5</sup> We hypothesized that aberrant miRNA expression could impact these processes in pancreatic cells, ultimately contributing to tumor initiation, promotion, and/or progression. In a preliminary work, we identified microRNA-21 (miR-21) as overexpressed in early pancreatic cancer lesions, pancreatic tumors, and pancreatic cancer-derived cell lines.<sup>6</sup> miR-21 is one of the most cited miRNA, and has emerged as the miRNA most frequently associated with poor outcome in cancer, including PDA.<sup>7</sup> In addition, miR-21 stands downstream in many oncogenic pathways<sup>8</sup> including but not restricted to activated *KRAS*<sup>6</sup> and *EGF* receptor<sup>6</sup> to target multiple tumor suppressors.<sup>8</sup> In theory, invalidation of miR-21 should (i) blunt many oncogenic pathways driving tumorigenesis, and (ii) relieve multiple antitumoral signals that could hinder tumor progression. As such, miR-21 is considered as a very promising therapeutic target for cancer, including PDA. However, most studies have been performed *in vitro*, and *in vivo* studies based on systemic or localized target delivery of anti-miR-21 are still lacking.<sup>8</sup>

In the present work, we asked whether depleting miR-21 may impede tumor proliferation *in vitro* and *in vivo* in a very aggressive preclinical model of PDA. Since a variety of human cancer cells including PDA have been shown to overexpress miR-21, development of a targeted therapeutic that would suppress oncogenic miR-21 would be a promising antitumor therapy against cancer.

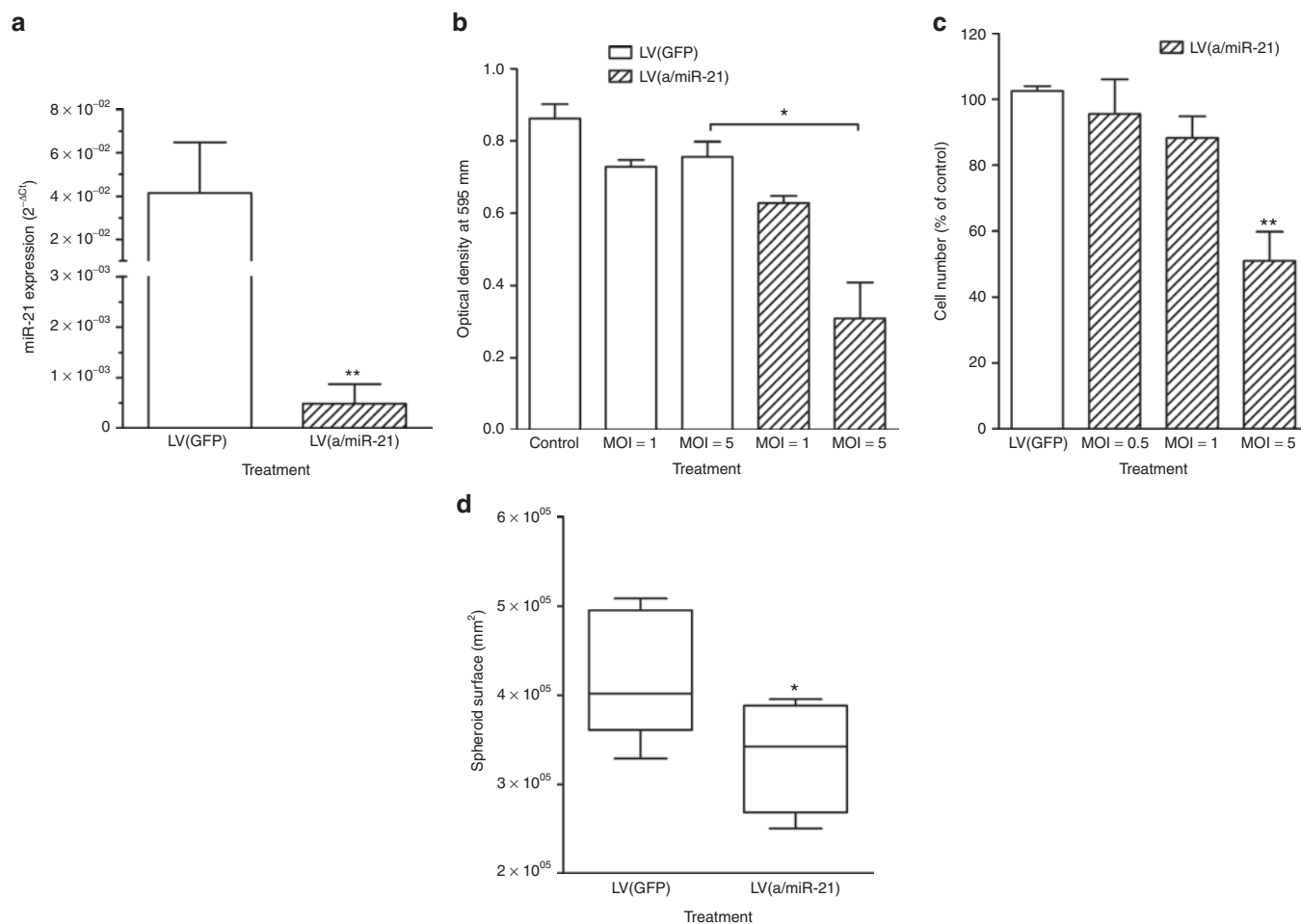


**Figure 1** *In vitro* targeting of miR-21 using lentiviral vectors decreases miR-21 cellular content and strongly inhibits PDA cell proliferation and viability. Mia PaCa-2 cells were transduced by LV(a/miR-21) encoding for miR-21 antisenses at the indicated MOI. Control cells were transduced with GFP-encoding lentiviral vectors, or left untransduced. **(a)** miR-21 expression was determined by qRT-PCR. Results, expressed as 2<sup>-ΔCt</sup>, are mean ± SEM of five independent experiments performed in duplicate. **(b)** Cell viability and **(c)** cell proliferation were determined 72 hours following transduction. Results are mean ± SEM of five independent experiments performed in triplicate. **(d)** Capan-2 cells were stably transduced with LV(a/miR-21). Control cells were stably transduced with LV(GFP). After 2 weeks in culture, spheroids surface was measured using ImageJ software. Results are mean ± SEM of three independent experiments of eight replicates. \**P* < 0.05; \*\**P* < 0.01. GFP, green fluorescent protein; LV, lentiviral vector; MOI, multiplicity of infection; PDA, pancreatic ductal adenocarcinoma; qRT-PCR, quantitative reverse transcriptase-PCR.

## RESULTS

### Targeting miR-21 inhibits PDA-derived cells proliferation

We previously demonstrated that the miRNA, miR-21 is overexpressed in early pancreatic cancer lesions, pancreatic tumors, and pancreatic cancer-derived cell lines.<sup>6</sup> To further study its function in PDA, we generated lentiviral vectors (LV) for the stable and permanent expression of RNA interference hairpins antisense to miR-21 (LV(a/miR-21)). These vectors transduced exponentially growing Mia PaCa-2 cells with high efficacy without selection (Supplementary Figure S1), to knockdown miR-21 expression (−95 ± 4%, *P* < 0.01, Figure 1a) as compared with control-transduced cells. Noteworthy, LV(a/miR-21) did not significantly impact the cellular levels of other miRNAs (Supplementary Figure S2). Consequently, PDA cell viability and cell proliferation were strongly antagonized, in a dose-dependent manner in response to LV(a/miR-21) treatment (Figure 1b,c, respectively). Inhibition of cell proliferation was maximal at 72 hours following

cell transduction (Supplementary Figure S3). In preclinical investigations, the multicellular tumor spheroid system has provided an appropriate *in vitro* system to evaluate and predict pancreatic tumor cells response to therapeutics.<sup>9</sup> Consequently, we generated spheroids of Capan-2 cells stably expressing miR-21 antisense. We found that targeting miR-21 significantly inhibited PDA tumor spheroids' growth as compared with control-transduced cells (Figure 1d). Taken together, we demonstrate that miR-21 is essential for the proliferation of PDA-derived tumor cells both in monolayer cultures and in three-dimensional models.

### miR-21 protects PDA-derived cells from apoptosis

We next investigated the molecular mechanisms involved in the antiproliferative effect consecutive to miR-21 depletion in PDA-derived cell lines. Mia PaCa-2 cells were transduced with different doses of LV(a/miR-21) and sampled for cell cycle analysis. Flow cytometric analysis of propidium iodide-stained cells showed that the pre-G0/G1 cell population significantly increases

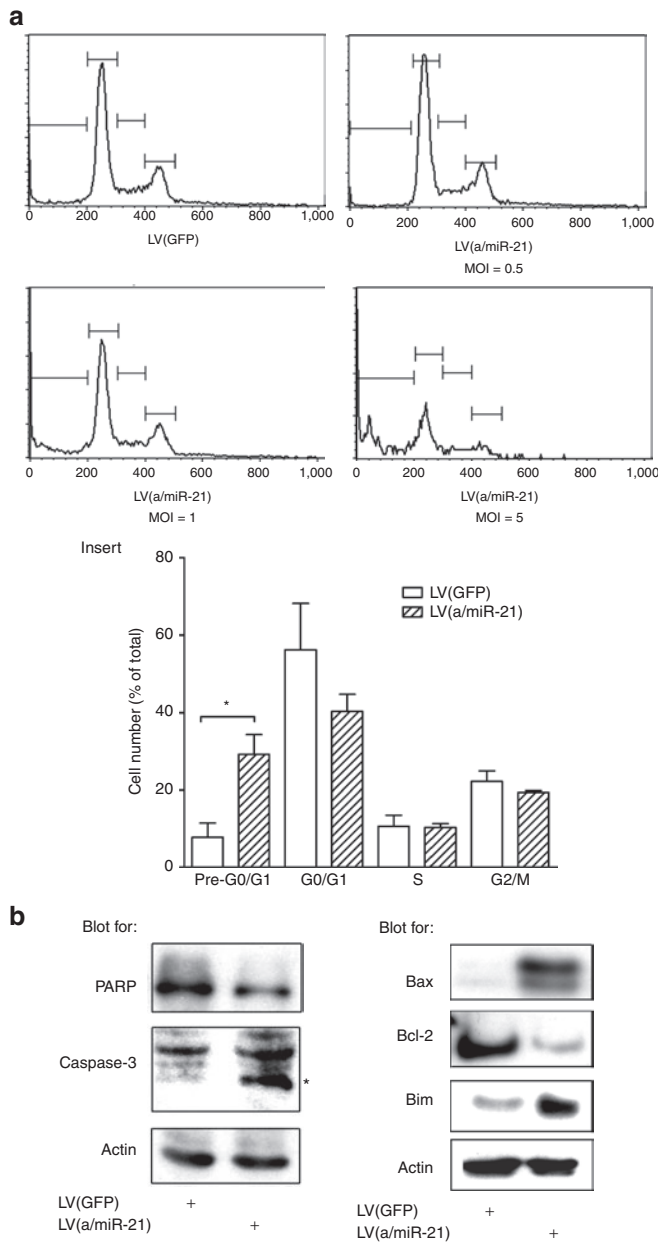


**Figure 2** miR-21 inhibition induces human PDA-derived cells' death by apoptosis via the mitochondrial pathway. Mia PaCa-2 cells were transduced by LV(a/miR-21) encoding for miR-21 antisenses at the indicated MOI. Control cells were transduced with GFP-encoding lentiviral vectors. **(a)** Flow cytometric analysis of propidium iodide-stained cells. Histograms are representative of three independent experiments. Insert: quantification of the DNA content distribution in each phase of the cell cycle. Results are mean  $\pm$  SEM of three independent experiments. \* $P < 0.05$ . **(b)** Western blot analysis of PARP and caspase-3 cleavage, and of Bax, Bcl-2, and Bim expression in the transduced cells. Results are representative of three independent experiments. GFP, green fluorescent protein; LV, lentiviral vector; MOI, multiplicity of infection; PDA, pancreatic ductal adenocarcinoma.

after exposure to LV(a/miR-21), as compared with control-transduced cells (Figure 2a). This effect was dose-dependent and maximal at multiplicity of infection = 5 ( $11.3 \pm 8.6$  fold increase,  $P < 0.05$ ; Figure 2a, insert). We next performed western blotting for caspase-3 and PARP in PDA-derived cell lines depleted for

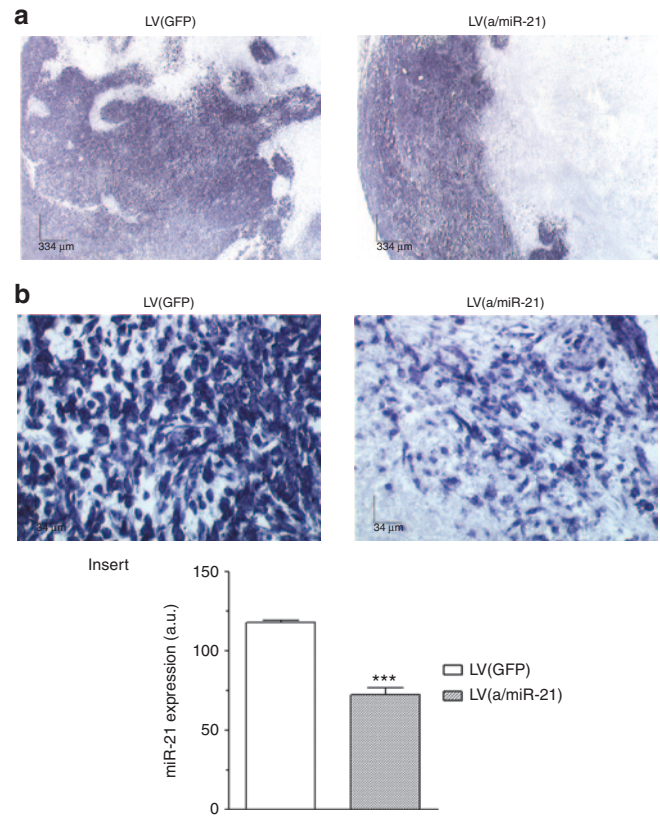


**Figure 3** Efficient knockdown of miR-21 in PDA tumors using lentiviral vectors. Pancreatic tissue was harvested 12 days following gene transfer for analysis of miR-21 expression by *in situ* hybridization. Results are representative of five different **(a)** low ( $\times 4$ ) or **(b)** high ( $\times 40$ ) power fields from three different tumors for each group. Insert: quantification of miR-21 expression using ImageJ software. Results are mean  $\pm$  SEM of 10 different fields from three different tumors for each group. \*\*\* $P < 0.005$ . a.u., arbitrary unit; GFP, green fluorescent protein; LV, lentiviral vector; PDA, pancreatic ductal adenocarcinoma.

miR-21. As shown in the left panel of the Figure 2b, transduction with LV(a/miR-21) induces caspase-3 and PARP cleavage in PDA-derived cell lines, as compared with control-transduced cells. In addition, we found that miR-21 knockdown resulted in Bcl-2 inhibition and induction of Bax and Bim by western blotting (Figure 2b, right panel) and immunofluorescence (data not shown). The latter findings support that miR-21 knockdown results in the activation of apoptosis through the mitochondrial pathway in PDA-derived cells.

### Noninvasive tracking of PDA tumor growth

We next generated a novel model of PDA for the noninvasive tracking of tumor growth based on the Lucia luciferase. Lucia belongs to the family of secreted luciferase, such as Gaussia luciferase, that can be sampled in the blood to monitor tumor growth and response to therapeutics.<sup>10</sup> Mia PaCa-2 cells expressing Lucia were plated in culture dishes and grown for 7 days. Lucia production was sampled in the culture medium and cells were counted. We found that (i) Lucia accumulated in the cell supernatant, and that (ii) Lucia levels were correlated to tumor cell number ( $R^2 = 0.91$ ) (Supplementary Figure S4a). We next demonstrated that

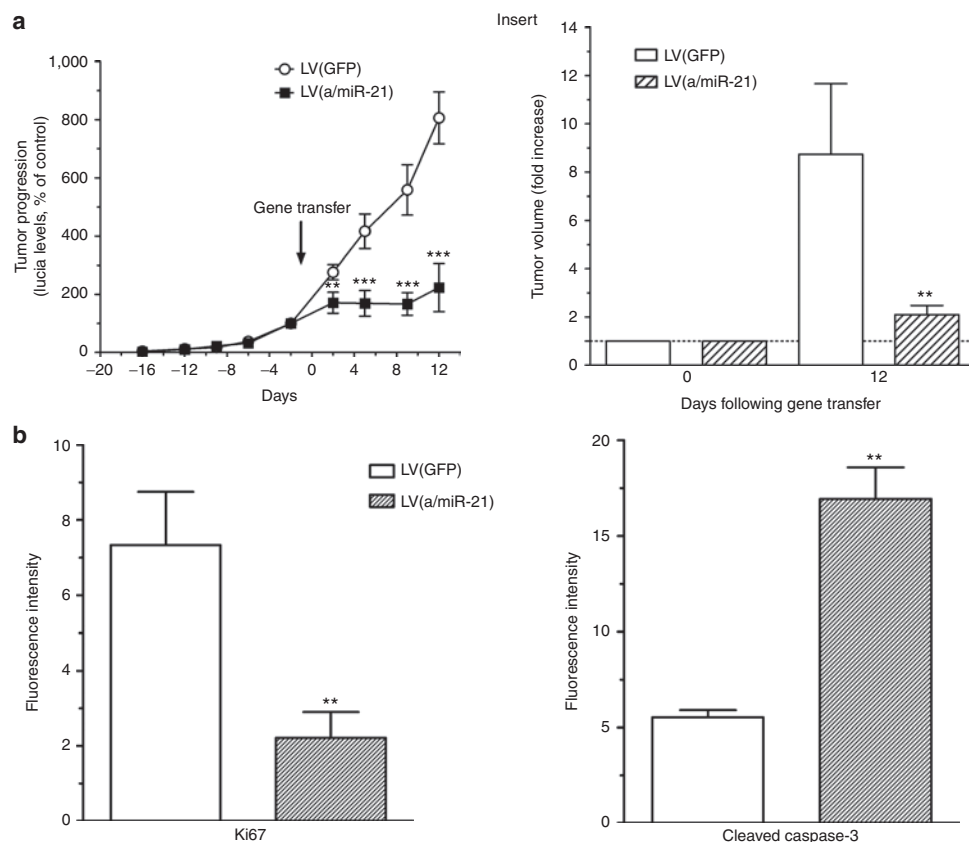


**Figure 4 Targeting miR-21 inhibits PDA tumor growth.** (a) Noninvasive monitoring of PDA tumor growth was performed for 34 days before and after intratumoral gene transfer. Results are mean  $\pm$  SEM of Lucia levels, expressed as % of day 0, in the serum of 12 animals per group. Insert: tumor volume was measured at day 0 and day 12 following intratumoral gene transfer using a caliper. Results are mean  $\pm$  SEM of tumor volume progression in 12 animals per group.  $**P < 0.01$ ;  $***P < 0.005$ . (b) Pancreatic tissue was harvested for the analysis of Ki67 (left) or cleaved caspase-3 (right) expression in the tumors by immunofluorescence. Results are mean  $\pm$  SEM of 15 different fields from three different tumors for each group.  $**P < 0.01$ . GFP, green fluorescent protein; LV, lentiviral vector; PDA, pancreatic ductal adenocarcinoma.

Mia PaCa-2 Lucia cells were as sensitive as parental Mia PaCa-2 cells to miR-21 depletion (Supplementary Figure S4b). Last, Lucia monitoring permits the noninvasive quantification of miR-21 knockdown inhibitory effect on PDA cells' proliferation, in a time and a dose-dependent manner (Supplementary Figure S4c).

We next engrafted Mia PaCa-2 Lucia cells in the pancreas of five severe combined immunodeficiency mice. Lucia was sampled from serum for 63 days. As expected, Lucia levels increased progressively in the blood of severe combined immunodeficiency mice with intrapancreatic tumors (Supplementary Figure S5a). However, tumor growth varied considerably between subjects. In addition, such slow-growing tumors may not be adequate for the preclinical testing of therapeutic regimens. Consequently, intrapancreatic tumors were removed, mechanically processed, cultured *ex vivo*, and injected in the pancreas of recipient mice. As shown in Supplementary Figure S5b and insert, tumor growth monitored by Lucia levels and tumor volume measurement was homogenous, to give rise to tumors 15 days following tumor cells implantation (Supplementary Figure S5b). Last, Lucia levels were correlated to tumor volume ( $R^2 = 0.85$ ) (Supplementary Figure S5c). Taken together, we demonstrate herein for the first time that Lucia blood assay can be used for the *ex vivo*, noninvasive, monitoring of PDA-derived cells tumor growth.

### ***In vivo* depletion of miR-21 strongly inhibits PDA tumor growth**

To assess the therapeutic efficacy of targeting miR-21 in PDA, LV(a/miR-21) were administrated with a single intratumoral injection 16 days following tumor induction, a time point at which animals typically have medium-sized tumors. Control tumors received LV(GFP). We observed no significant variations in body weight of animals receiving LVs, underscoring the safety of targeting oncogenic miRNA using LVs (Supplementary Figure S6). Pancreatic tissue was harvested 2 weeks later for analysis of miRNA expression. As expected, human tumors transduced with LV(GFP) exhibited high-level expression of miR-21, both in tumor cells and their microenvironment (Figure 3). On the other hand, LV(a/miR-21) delivery resulted not only in histological evidence of tumor necrosis but also inhibition of miR-21 expression in tumor cells (Figure 3b and insert). These data demonstrate that LV(a/miR-21) provides an effective means to target miR-21 in pancreatic tumors.

We next monitored orthotopic pancreatic tumors progression using blood Lucia assay following LV(GFP) or LV(a/miR-21) intratumoral administration. Strikingly, the growth of this very aggressive tumor model was stopped by day 2 up to day 12 following *in vivo* depletion of miR-21, compared with green fluorescent protein (GFP)-expressing LVs (Figure 4a). Animals were killed

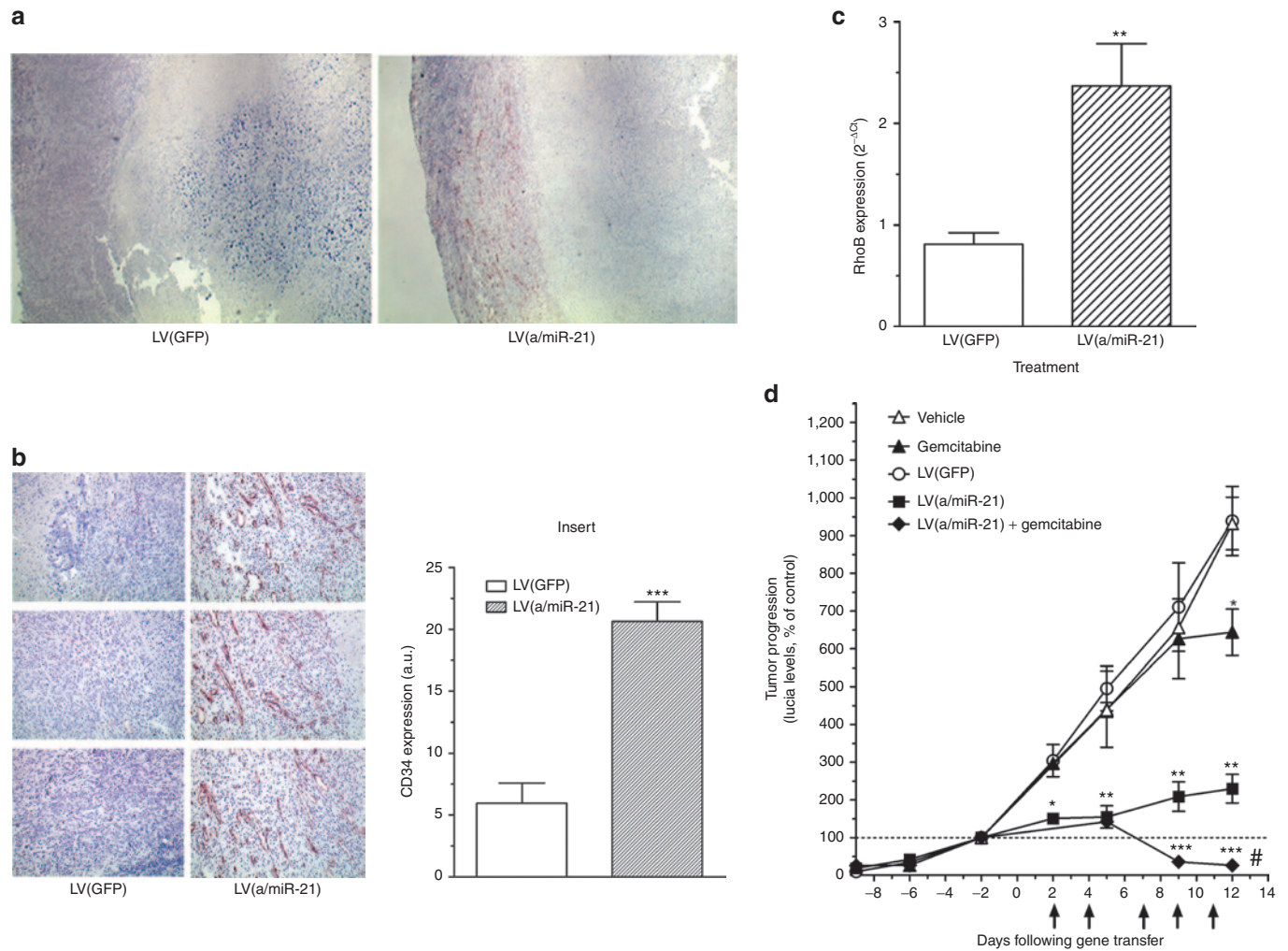


**Figure 5 Targeting miR-21 induces tumor angiogenesis and potentiates gemcitabine antitumor effect.** Pancreatic tissue was harvested 12 days following gene transfer for analysis of CD34 expression by immunohistochemistry. Results are representative of (a) 5 low and (b) 15 high power fields from three different tumors per group. Insert: quantification of CD34 expression using Image J software. Results are mean  $\pm$  SEM of 15 different low power fields from three different tumors for each group.  $***P < 0.005$ . (c) Total RNA was extracted from tumors and analyzed for RhoB expression by qRT-PCR. Results, expressed as  $2^{-\Delta Ct}$ , are mean  $\pm$  SEM of three different tumors for each group. (d) Lucia was quantified in mice serum every 2–3 days during the course of the experiment. Arrows indicate the intraperitoneal injection of gemcitabine. Results are mean  $\pm$  SEM of Lucia levels, expressed as % of day 0, in the serum of 5–10 animals per group.  $*P < 0.05$ ;  $**P < 0.01$ ;  $***P < 0.005$ ,  $\#P < 0.005$  comparing gemcitabine versus gemcitabine + LV(a/miR-21) or LV(a/miR-21) versus gemcitabine + LV(a/miR-21). a.u., arbitrary unit; GFP, green fluorescent protein; LV, lentiviral vector; qRT-PCR, quantitative reverse transcriptase-PCR.

and tumor burden was assessed 2 weeks following intratumoral gene transfer. Animals treated with control vectors developed fulminant disease as tumor volume increased by more than eightfold during the course of the experiment (Figure 4a, insert). In contrast, LV(a/miR-21)-treated animals were dramatically protected, exhibiting only weak tumor progression ( $2.09 \pm 0.4$  fold increase). In addition, we observed (i) markedly reduced Ki67 staining and (ii) induction of apoptosis as measured by caspase-3 cleavage in tumors following administration of LV(a/miR-21) (Figure 4b). We conclude that targeting miR-21 uniformly diminished disease progression of experimental pancreatic adenocarcinoma.

### Targeting miR-21 induces tumor angiogenesis

miR-21 is one of the few miRNAs involved in angiogenesis regulation,<sup>11,12</sup> and acts as an inhibitor of endothelial cell proliferation

and migration in a mouse model of choroidal neovascularization.<sup>11</sup> We asked whether pancreatic tumor vascularization was affected following LV(a/miR-21) treatment. LV(GFP)-transduced pancreatic tumors were weakly vascularized (Figure 5a,b). However, miR-21 depletion resulted in the massive induction of vessels surrounding the tumor ( $4 \pm 1.1$  fold increase,  $P < 0.005$ ; Figure 5b, insert). Interestingly, peripheral blood vessels also demonstrated a marked reduction in miR-21 levels following LV(a/miR-21) gene transfer (Supplementary Figure S7). To investigate the mechanisms through which miR-21 down-expression results in pancreatic tumor angiogenesis, we examined functional targets of this miRNA.<sup>8,11</sup> While the expression of Sprouty-1 and Sprouty-2 remained unchanged between LV(GFP)- and LV(a/miR-21)-treated tumors (data not shown), RhoB expression greatly increased following miR-21 depletion (Figure 5c), as previously

described in other models.<sup>11</sup> Altogether, these data document that miR-21 represses the expression of RhoB, providing one mechanism through which targeting this miRNA enhances PDA tumor angiogenesis.

### Combining miR-21 targeting and chemotherapeutic treatment provokes pancreatic tumor regression

Despite its contested efficacy in preclinical models and clinical trials for PDA patients, gemcitabine became the standard treatment for advanced disease 15 years ago after showing superiority over fluorouracil. Since then, many phase III trials of newer cytotoxic or biologic agents combined with gemcitabine have not shown any survival improvement compared with gemcitabine alone.<sup>2</sup> To assess whether targeting miR-21 may translate into clinical practice to manage PDA, we compared the efficacy of our approach with standard gemcitabine treatment. Consequently, LV(GFP) and LV(a/miR-21) vectors were injected into exponentially growing pancreatic tumors. In parallel, high dosage of gemcitabine (125 mg/kg) was administered twice weekly by intraperitoneal injection. Blood samples were collected every 2–3 days during the course of the experiment. We found that gemcitabine slightly inhibited PDA tumor progression, as compared with vehicle ( $-21\%$ ,  $P < 0.05$ , **Figure 5d**). On the other hand, miR-21 depletion strongly inhibited PDA tumor growth, as compared with LV(GFP)-transduced tumors ( $-75\%$ ,  $P < 0.01$ , **Figure 5d**).

Because the data presented herein support that depletion of miR-21 stimulates angiogenesis in this experimental model of PDA, we hypothesized that targeting miR-21 may augment tumor drug delivery to enhance the efficacy of systemic therapies. The results presented **Figure 5d** demonstrate that combining gemcitabine treatment and transduction with LV(a/miR-21) stopped tumor progression (**Figure 5d**) and induced tumor shrinkage ( $-40 \pm 5\%$ ,  $P < 0.01$  data not shown), as compared with control tumors. Thus, we demonstrate for the first time that (i) targeting miR-21 is more effective than standard chemotherapeutic treatment to inhibit PDA tumor growth, and that (ii) combining both therapeutic approaches provokes tumor regression in this very aggressive experimental model of pancreatic cancer.

## DISCUSSION

PDA is a highly heterogeneous disease.<sup>13</sup> Large-scale genetic analysis recently shed light on the numerous exomic alterations detected in this cancer in diverse signaling pathways.<sup>14</sup> In addition, primary tumors are intrinsically heterogeneous, and specific cellular subclones can also be identified in metastasis.<sup>15</sup> Interestingly, the type and number of genomic rearrangements in DNA vary considerably between patients, while they seem to occur early during tumor development.<sup>16</sup> This heterogeneity is believed to be a major clinical obstacle to the successful treatment of PDA.

PDA has developed sophisticated networks of biological activities to maintain self-sufficiency in growth signal, resistance to endogenous antiproliferative signals, evasion from apoptosis, limitless replicative potential, and tissue invasion and metastasis. Noteworthy, miRNAs are demonstrated to participate in each one of these processes. This feature renders miRNA highly appealing as therapeutic target, considering that modulation of a single miRNA may affect many pathways simultaneously to achieve

clinical benefit. Such approach is likely to reduce the emergence of resistant clones since many concomitant mutations would be required to subvert the effects of miRNA expression modulation.

Alterations in miRNA expression are not exceptional but rather common in human cancer.<sup>5</sup> We were among the first to demonstrate that miR-21, the miRNA which is most frequently associated with poor outcome in human cancer,<sup>7</sup> is expressed early during pancreatic carcinogenesis.<sup>6</sup> Compelling evidences indicate that miR-21 participates in many cancerous pathways, such as cancer cell proliferation, migration, invasion, metastasis, and resistance to cytotoxic chemotherapeutic agents.<sup>8</sup> In PDA, inhibition of miR-21 decreases proliferation, matrigel invasion, and chemoresistance to gemcitabine, *in vitro*.<sup>17</sup> Taken together, these findings stem for the use of miR-21 as therapeutic target in PDA.

To date, most translational *in vivo* studies targeting miRNAs faced several concerns that need to be addressed before advancing to medical practice.<sup>5</sup> In the present study, we found that locked nucleic acid antagonists successfully inhibited miR-21 function *in vitro*, but failed to target this miRNA *in vivo* (data not shown). Our findings strongly suggest that the lack of stability and the incapacity of these molecules to overcome the tumor microenvironment are major hurdles for direct miRNA-based therapy of pancreatic tumors. While the use of synthetic oligonucleotide inhibitors is promising and will remain a fruitful area of investigation, rapid progress must be made to achieve effective delivery of miRNA inhibitors in target tissues. Consequently, we selected viral-based vectors originally developed for gene therapy to express anti-miR-21 molecular sponges. We recently demonstrated that pancreatic cancer gene therapy strongly relies on the delivery vector.<sup>18–20</sup> From our expertise, HIV-1-based LVs outshine other vectors (PEI, adenovirus, SV40...) in delivering therapeutic genes into pancreatic cancer cells, *in vitro* and *in vivo*.<sup>18</sup> In addition, LVs have proven to be effective to achieve stable miRNA knockdown, *ex vivo*.<sup>21</sup> The results described herein demonstrate for the first time that miRNA antagonists are highly efficient in targeting miR-21, when delivered by LVs both *in vitro* and *in vivo*, without impacting on endogenous miRNA biogenesis. However, it is mandatory to underline the possible genotoxicity associated with the use of LVs.<sup>22</sup> In our study, the delivered material is integrated in the host DNA with an unpredictable risk of insertional mutagenesis, activation of proto-oncogenes in healthy cells or even generation of aberrant transcripts.<sup>23</sup> Consequently, we are now designing integrase-deficient LVs for the safe and efficient gene delivery of miRNA inhibitors in PDA-derived cells.

We found that tumor cell proliferation and tumor progression are strongly inhibited following miR-21 depletion in a very aggressive model of pancreatic cancer. Interestingly, miR-21 inhibition also decreased PDA-derived tumor cells proliferation in three-dimensional models, strongly suggesting that this miRNA may favor the tumor-initiating capacity of pancreatic cancer stem cells. Although the molecular basis of this inhibitory effect requires further investigation, we demonstrate herein that miR-21 depletion provokes PDA cell death by apoptosis as determined by PARP and caspase-3 cleavage assays. We further demonstrate that anti-miR-21 treatment is associated with downregulation of Bcl-2 and upregulation of Bax expression,<sup>24,25</sup> respectively, and provide for the first time evidences of Bim induction in response

to miR-21 depletion in cancer cells. Our results are in agreement with previous reports suggesting that miR-21 is an oncogene that plays a key role in resisting programmed cell death in cancer cells, particularly through the mitochondrial pathway.<sup>8</sup> In the present study, the expression levels of PTEN and PDCD4, two canonical targets of miR-21, were not altered following miR-21 depletion in both Mia PaCa-2 and Capan-2 cells (data not shown). While protein levels of PTEN are increased in PDA-derived HS766T cells by antisense to miR-21,<sup>26</sup> direct targeting of this tumor suppressor gene by miR-21 in PDA remains to be fully characterized.<sup>8</sup> Studies are undergoing to identify direct targets of miR-21 in PDA-derived cells.

We next established the principle that targeting miR-21 severely impairs pancreatic tumor growth. We used for the first time secreted luciferase as a marker for the noninvasive monitoring of PDA growth in mice. We demonstrated that blood levels of Lucia luciferase produced by PDA cells perfectly correlates with caliper measurement of orthotopic tumors volume. Unlike commonly used measuring devices, Lucia levels may be a valuable indicator of tumor viability. Using this unique model, we demonstrate that therapeutic delivery of miRNA inhibitors in highly proliferating and very aggressive pancreatic tumors can result in tumor growth inhibition. The dramatic sensitivity of the tumor cells to the specific reduction in miR-21 levels underscores the contribution of gain-of-function of this miRNA to pancreatic tumorigenesis. Tumor cells stopped to proliferate and underwent apoptosis following miR-21 depletion. We found that our approach surpasses the therapeutic efficacy of standard treatments for this disease. What remains to be investigated is whether miR-21 is a rationale target that may have beneficial effects on metastatic disease.

Surprisingly, we found that targeting miR-21 increases the number of blood vessels in the surrounding tissue. In order to elaborate a putative mechanism for miR-21 targeting to induce angiogenesis, we focused on the identification of the targets of this miRNA both in the tumor and its microenvironment. Indeed, we found that peripheral blood vessels also demonstrated a marked reduction in miR-21 following LV(a/miR-21) gene transfer. Our results support a role for the Rho GTPase RhoB, a key regulator of angiogenesis through the modulation of vascular permeability, extracellular matrix remodeling, migration and proliferation of endothelial cells, in the proangiogenic process following miR-21 depletion. Interestingly, RhoB has also been extensively described in tumor cells where it seems to act as a tumor suppressor gene. Whether RhoB may also participate in the inhibition of tumor cell proliferation following miR-21 targeting remains to be investigated.

Based on the finding that miR-21 silencing enhances blood vessel growth, we hypothesized that depleting miR-21 may provoke better drug delivery in pancreatic tumors. We demonstrate that gemcitabine and miR-21 targeting are synergistic, as this co-treatment led to a very impressive antitumoral effect that is rarely achieved in this experimental model. Taken together, we demonstrate that miR-21 is a suitable therapeutic target in PDA and that combining epigenetic silencing and chemotherapeutic treatment induce unexpected pancreatic tumor regression.

The present study design involved the treatment of existing tumors with miR-21 inhibitors, a paradigm closely related to

the clinical scenarios in which this approach may be employed. Indeed, we are currently conducting a first-in-man phase I gene therapy clinical trial in 24 patients diagnosed with advanced pancreatic cancer (Thergap clinical trial, ClinicalTrials.gov identifier NCT01274455). We demonstrated during this trial, the feasibility and the safety of transfecting PDA tumors with nonviral vectors using endoscopic ultrasound (data not shown). While groundbreaking, this unique clinical trial will strongly benefit from the characterization of new delivery vehicles and new molecular targets that may help alleviate the dismal prognosis of this disease. Because miR-21 is overexpressed in most human tumors,<sup>7</sup> therapeutic delivery of miR-21 antagonists may still be beneficial for a large number of cancers for which no cure is available. While there clearly remains significant work to be done, our findings highlight the therapeutic promise of this approach.

## MATERIALS AND METHODS

**Cell culture and generation of multicellular tumor spheroids.** Human PDA-derived Capan-2 cells were grown in RPMI medium supplemented with 10% fetal calf serum, L-glutamine, antibiotic and antimycotic cocktail (Life Technologies SAS, St Aubin, France) and Plasmocin (Cayla-INVIVOGEN EUROPE, Toulouse, France). Mia PaCa-2 cells were grown in Dulbecco's modified Eagle's medium containing 4.5 g/l glucose (Invitrogen), 10% fetal calf serum, L-glutamine, antibiotics, Fungizone, and Plasmocin (InvivoGen). Spheroids were prepared following the "hanging-drop method" with minor modifications.<sup>9</sup> Briefly, 20  $\mu$ l drops containing 500 Capan-2 cells were suspended from the lids of 24-well culture dishes and transferred to 24-well culture dishes, base-coated with agar for 2 weeks. Cell lines and spheroids were grown in a humidified incubator at 37°C in 5% CO<sub>2</sub>.

**Cell cycle analysis by flow cytometry.** Mia PaCa-2 cells were collected, rinsed once in phosphate-buffered saline (PBS) and fixed in ice-cold 70% ethanol overnight at 4°C. Cells were collected by centrifugation at 1,000g and rinsed with PBS. Cells were incubated with propidium iodide following manufacturer's recommendation (Invitrogen). Cell cycle distribution was determined using BD FACS Calibur apparatus and Cell quest pro software (Becton Dickinson, Le Pont de Claix, France).

**Gene expression analysis.** Total RNA was isolated from cell lines with TRIzol Reagent (Invitrogen) according to supplier's instructions and RNA concentration was measured with the ND-1000 NanoDrop spectrophotometer (Nanodrop, Wilmington, DE). miRNAs were quantified from 1  $\mu$ g total RNA using the miScript PCR System (Qiagen, COURTABOEUF, France). U6 and 5S RNAs were used as internal controls. cDNA samples were diluted 1 into 100 for miRNA detection or U6 and 1 into 10,000 for 5S RNA detection. RhoB was quantified as reported previously.<sup>11</sup> DNA samples were diluted 1 into 100 for RhoB detection or U6 and 1 into 1,000 for GAPDH and actin RNA detection. Duplicate quantitative reverse transcriptase-PCR assays were carried out in a StepOnePlus Real-Time PCR System (Life Technologies SAS) with SYBR Green PCR Master Mix. Relative amounts of were calculated by the comparative threshold cycle (CT) method as  $2^{-\Delta CT}$ , where  $\Delta CT = CT$  (gene of interest) – CT (geometric mean of control genes).

**Cell viability and cell proliferation analysis.** Mia PaCa-2 cells were seeded at  $6 \times 10^3$  cells per well in a 96-well dish and grown in complete medium. Twenty-four hours later, cells were transduced with LV(a/miR-21) indicated multiplicity of infection. Control cells were transduced with LV(GFP). Number of viable cells was determined by colorimetric method using CellTiter 96 AQueous Non-Radioactive Cell Proliferation Assay (Promega, Charbonnieres, France) according to manufacturer's instructions 72 hours following transduction. Cell proliferation assays

were performed in 35-mm dishes.  $50 \times 10^3$  Mia PaCa-2 cells were cultured in complete medium for 24 hours (2 ml per dish). The next day, cells were transduced with LV(a/miR-21) at the indicated multiplicity of infection (**Supplementary Materials and Methods**). Control cells were transduced with LV(GFP). Cell growth was measured at days 1, 2, and 3 following transduction by cell counting using a Coulter counter model ZM (Beckman Coulter, Roissy, France). All experiments were conducted with different batches of LVs. Transduced cells were not selected in this study.

**Western blotting.** Proteins were extracted from transduced cells or tumors, resolved on SDS-polyacrylamide gels, and transferred to nitrocellulose membrane. After room temperature blocking for 1 hour, blots were incubated overnight at 4°C with antibodies purchased from Cell signaling Technology (St Quentin Yvelines, France) diluted according to the manufacturer's recommendations. Secondary horseradish peroxidase-conjugated antibodies (dilution 1:10,000; Perbio Science, Brebières, France) were added, and blots were incubated for 1 hour at room temperature. Immunoreactive proteins were visualized using ECL immunodetection (Immobilon; Millipore, Billerica, MA).

**Immunostaining for Ki67, CD34, and cleaved caspase-3.** Mia PaCa-2 tumors were harvested and fixed in formalin. Four micrometer thick sections were prepared from paraffin-embedded sections and rehydrated. Following antigen retrieval, sections were incubated for 10 minutes in Protein Block, Serum-free reagent to reduce background staining (DakoCytomation). Slides were next incubated overnight at 4°C with anti-Ki67 or CD34 antibodies (DakoCytomation, Les Ulis, France; dilution: 1:100), or cleaved caspase-3 antibody (Cell signaling Technology; dilution: 1:250) developed in rabbits. Antibody incubations were done in Antibody diluents (DakoCytomation). For CD34 staining, slides were washed and incubated in 3% H<sub>2</sub>O<sub>2</sub> for 30 minutes at room temperature for endogenous peroxidase inhibition. Slides were quickly rinsed in distilled water, washed twice in PBS, and incubated for 30 minutes at room temperature with Envision+ system-HRP (DakoCytomation). After washing in distilled water, slides were incubated in AEC+ reagent and counterstained with Mayer's hematoxylin. For Ki67 and cleaved caspase-3 staining, slides were washed and incubated for 1 hour, protected from light with Goat anti-rabbit CY3 conjugated secondary antibodies (1:50; Jackson ImmunoResearch, Suffolk, UK). After washing in PBS, slides were mounted with Vectashield containing DAPI (Vector Laboratories, Burlingame, CA). Immunostaining was recorded with an optical microscope, and quantified using VisioLab2000 image analyzer (Biocom, Les Ulis, France).

**In situ hybridization for miR-21.** *In situ* hybridization for miR-21 was conducted as described elsewhere.<sup>6</sup> Briefly, *in situ* hybridization was performed on PDA tumors using LNA probes for miR-21 (Exiqon, Vedbaek, Denmark). Paraffin-embedded tumors were deparaffinized, treated by proteinase K, and fixed in paraformaldehyde. Digoxigenin-labeled LNA probe was hybridized overnight. Slides were rinsed and incubated with anti-digoxigenin Fab fragment (Roche diagnostics, Meylan, France) overnight. The detection reaction was performed using NBT/BNI Ready-to-use tablets (Roche diagnostics) and slides were mounted with cover slip using Glyceragel mounting medium (DakoCytomation). Slides were observed with a Nikon E400 optical microscope, coupled to an image analyzer (VisioLab2000; Biocom). For each sample, 15 fields were analyzed.

**Experimental protocol.** Sixteen days following implantation of Mia PaCa-2 Lucia F1 cells (**Supplementary Materials and Methods**), tumors measured ~400 mm<sup>3</sup> in volume and mice were randomized into the following treatment groups ( $n = 12$ ) regardless of the level of bioluminescence measured in the serum: (i) transduction with 150 ng of p24 of LV(GFP); (ii) transduction with 150 ng of p24 of LV(a/miR-21) in a level 2 animal safety facility as previously described.<sup>18</sup> For the gemcitabine study, we used five animals per group. Gemcitabine (125 mg/kg) was administrated twice weekly by intraperitoneal injection. Blood samples were collected every

2–3 days during the course of the experiment. The animals were killed 12 days after gene transfer and the tumor tissue was (i) formalin-fixed and paraffin-embedded for immunohistochemistry and routine hematoxylin and eosin staining was performed, and (ii) snap frozen in liquid nitrogen and stored at –80°C. Hematoxylin and eosin staining confirmed the presence of tumor(s) in each pancreas. Lucia production was measured in 5 µl of serum using coelenterazine (50 µmol/l) as a substrate.

**Statistical analysis.** Results are expressed as mean ± SE. Data were compared by unpaired *t*-tests ( $*P < 0.05$ ,  $**P < 0.01$ ;  $***P < 0.005$ ) or one-way analysis of variance with Bonferroni's multiple comparison test ( $*P < 0.005$ ) using Graphpad Prism software (Graphpad Software, La Jolla, CA).  $P < 0.05$  was considered significant.

## SUPPLEMENTARY MATERIAL

**Figure S1.** Lentiviral vectors transduce human PDA-derived cell lines with high efficacy.

**Figure S2.** Targeting miR-21 does not impact on other cellular miRNA expression.

**Figure S3.** Kinetics of inhibition of cell proliferation following targeting of miR-21 in PDA-derived cells.

**Figure S4.** Lucia expression correlates with tumor cell proliferation and response to treatment.

**Figure S5.** Noninvasive tracking of pancreatic tumor growth using Lucia luciferase.

**Figure S6.** Tumor growth and intrapancreatic injection of lentiviral vectors are well tolerated in SCID mice.

**Figure S7.** miR-21 is downregulated in peripheral blood vessels following LV(a/miR-21) gene transfer.

## Materials and Methods.

## ACKNOWLEDGMENTS

This work was supported by grants from INSERM, Region Midi-Pyrenees (10051310), and la Fondation de l'Avenir (ET2-656). F.S. was supported by a postdoctoral fellowship from the Innabiosanté Foundation.

## REFERENCES

- Jemal, A, Bray, F, Center, MM, Ferlay, J, Ward, E and Forman, D (2011). Global cancer statistics. *CA Cancer J Clin* **61**: 69–90.
- Torrisani, J, Bournet, B, Cordelier, P and Buscail, L (2008). [New molecular targets in pancreatic cancer]. *Bull Cancer* **95**: 503–512.
- Conroy, T, Desseigne, F, Ychou, M, Bouché, O, Guimbaud, R, Bécouarn, Y *et al.*; Groupe Tumeurs Digestives of Unicancer; PRODIGE Intergroup. (2011). FOLFIRINOX versus gemcitabine for metastatic pancreatic cancer. *N Engl J Med* **364**: 1817–1825.
- Delpu, Y, Hanoun, N, Lulka, H, Sicard, F, Selves, J, Buscail, L *et al.* (2011). Genetic and epigenetic alterations in pancreatic carcinogenesis. *Curr Genomics* **12**: 15–24.
- Iorio, MV and Croce, CM (2012). MicroRNA dysregulation in cancer: diagnostics, monitoring and therapeutics. A comprehensive review. *EMBO Mol Med* **4**: 143–159.
- du Rieu, MC, Torrisani, J, Selves, J, Al Saati, T, Souque, A, Dufresne, M *et al.* (2010). MicroRNA-21 is induced early in pancreatic ductal adenocarcinoma precursor lesions. *Clin Chem* **56**: 603–612.
- Nair, VS, Maeda, LS and Ioannidis, JP (2012). Clinical outcome prediction by microRNAs in human cancer: a systematic review. *J Natl Cancer Inst* **104**: 528–540.
- Pan, X, Wang, ZX and Wang, R (2010). MicroRNA-21: a novel therapeutic target in human cancer. *Cancer Biol Ther* **10**: 1224–1232.
- Dufau, I, Frongia, C, Sicard, F, Dedieu, L, Cordelier, P, Ausseil, F *et al.* (2012). Multicellular tumor spheroid model to evaluate spatio-temporal dynamics effect of chemotherapeutics: application to the gemcitabine/CHK1 inhibitor combination in pancreatic cancer. *BMC Cancer* **12**: 15.
- Chung, E, Yamashita, H, Au, P, Tannous, BA, Fukumura, D and Jain, RK (2009). Secreted Gaussia luciferase as a biomarker for monitoring tumor progression and treatment response of systemic metastases. *PLoS ONE* **4**: e8316.
- Sabatel, C, Malvaux, L, Bovy, N, Deroanne, C, Lambert, V, Gonzalez, ML *et al.* (2011). MicroRNA-21 exhibits antiangiogenic function by targeting RhoB expression in endothelial cells. *PLoS ONE* **6**: e16979.
- Wang, S and Olson, EN (2009). AngiomiRs—key regulators of angiogenesis. *Curr Opin Genet Dev* **19**: 205–211.
- Costello, E, Greenhalf, W and Neoptolemos, JP (2012). New biomarkers and targets in pancreatic cancer and their application to treatment. *Nat Rev Gastroenterol Hepatol* **9**: 435–444.
- Jones, S, Zhang, X, Parsons, DW, Lin, JC, Leary, RJ, Angenendt, P *et al.* (2008). Core signaling pathways in human pancreatic cancers revealed by global genomic analyses. *Science* **321**: 1801–1806.
- Yachida, S, Jones, S, Bozic, I, Antal, T, Leary, R, Fu, B *et al.* (2010). Distant metastasis occurs late during the genetic evolution of pancreatic cancer. *Nature* **467**: 1114–1117.



16. Campbell, PJ, Yachida, S, Mudie, LJ, Stephens, PJ, Pleasance, ED, Stebbings, LA *et al.* (2010). The patterns and dynamics of genomic instability in metastatic pancreatic cancer. *Nature* **467**: 1109–1113.
17. Moriyama, T, Ohuchida, K, Mizumoto, K, Yu, J, Sato, N, Nabae, T *et al.* (2009). MicroRNA-21 modulates biological functions of pancreatic cancer cells including their proliferation, invasion, and chemoresistance. *Mol Cancer Ther* **8**: 1067–1074.
18. Ravet, E, Lulka, H, Gross, F, Casteilla, L, Buscail, L and Cordelier, P (2010). Using lentiviral vectors for efficient pancreatic cancer gene therapy. *Cancer Gene Ther* **17**: 315–324.
19. Carrere, N, Vernejoul, F, Souque, A, Asnacios, A, Vaysse, N, Pradayrol, L *et al.* (2005). Characterization of the bystander effect of somatostatin receptor sst2 after *in vivo* gene transfer into human pancreatic cancer cells. *Hum Gene Ther* **16**: 1175–1193.
20. Cordelier, P, Bienvenu, C, Lulka, H, Marrache, F, Bouisson, M, Openheim, A *et al.* (2007). Replication-deficient rSV40 mediate pancreatic gene transfer and long-term inhibition of tumor growth. *Cancer Gene Ther* **14**: 19–29.
21. Gentner, B, Schira, G, Giustacchini, A, Amendola, M, Brown, BD, Ponzoni, M *et al.* (2009). Stable knockdown of microRNA *in vivo* by lentiviral vectors. *Nat Methods* **6**: 63–66.
22. Durand, S and Cimarelli, A (2011). The inside out of lentiviral vectors. *Viruses* **3**: 132–159.
23. Moiani, A, Paleari, Y, Sartori, D, Mezzadra, R, Miccio, A, Cattoglio, C *et al.* (2012). Lentiviral vector integration in the human genome induces alternative splicing and generates aberrant transcripts. *J Clin Invest* **122**: 1653–1666.
24. Shi, L, Chen, J, Yang, J, Pan, T, Zhang, S and Wang, Z (2010). MiR-21 protected human glioblastoma U87MG cells from chemotherapeutic drug temozolomide induced apoptosis by decreasing Bax/Bcl-2 ratio and caspase-3 activity. *Brain Res* **1352**: 255–264.
25. Si, ML, Zhu, S, Wu, H, Lu, Z, Wu, F and Mo, YY (2007). miR-21-mediated tumor growth. *Oncogene* **26**: 2799–2803.
26. Park, JK, Lee, EJ, Esau, C and Schmittgen, TD (2009). Antisense inhibition of microRNA-21 or -221 arrests cell cycle, induces apoptosis, and sensitizes the effects of gemcitabine in pancreatic adenocarcinoma. *Pancreas* **38**: e190–e199.